

Propagation of subcycle pulses in a two-level medium: Area-theorem breakdown and pulse shape

Denis V. Novitsky*

*B. I. Stepanov Institute of Physics, National Academy of Sciences of Belarus,
Nezavisimosti Avenue 68, BY-220072 Minsk, Belarus*

(Dated: October 20, 2018)

We solve the problem of ultrashort pulse propagation in a two-level medium beyond the rotating-wave (RWA) and slowly-varying-envelope approximations. The method of solution is based on the Maxwell–Bloch equations represented in the form that allows one to switch between RWA and general (non-RWA) cases in the framework of a single numerical algorithm. Using this method, the effect of a subcycle pulse (containing less than a single period of field oscillations) on the two-level medium was analyzed. It is shown that for such short pulses, the clear breakdown of the area theorem occurs for the pulses of large enough area. Moreover, deviations from the area theorem appear to be strongly dependent on the pulse shape that cannot be observed for longer few-cycle pulses.

PACS numbers: 42.65.Re, 42.65.Sf, 42.50.Md, 42.65.Pc

I. INTRODUCTION

As the light pulses produced with modern laser techniques become shorter, so that their duration becomes comparable with the period of optical field oscillation, the necessity of an adequate theoretical description of the propagation of such ultrashort pulses in different systems tends to be more and more obvious. One of the basic models of an optical medium is a two-level medium, the fundamental model of a resonantly absorbing medium. The case of pulses containing only a few cycles of field oscillations implies that the analysis of the pulse dynamics in the two-level medium should be carried out beyond the popular and standard approximations – the slowly-varying-envelope approximation (SVEA) and the rotating-wave approximation (RWA). The study of few-cycle pulse propagation under such generalized conditions (beyond SVEA and RWA) has been under way since the mid 1990s and has given a number of important results. For example, the main effects previously known, such as self-induced transparency (SIT), 2π soliton formation, and 4π pulse splitting, were reported to be valid for the few-cycle pulse though some additional features in the dynamics of the two-level medium were found as well [1–3]. Among other results one can mention the spectral transformations due to the intrapulse four-wave mixing [2], the local-field effects on the few-cycle pulse propagation [4, 5], the generation of a single-cycle soliton in a subwavelength structure consisting of the two-level medium [6], and the creation of the quasisolitons in a waveguide-like resonantly absorbing nanostructure [7]. The most recent achievements include the effects of the chirp [8–10] and the so-called counter-rotating terms in the Bloch equations [11] on femtosecond pulse propagation.

In this paper we study the validity of the area theorem for even shorter (subcycle) pulses. Previously Hughes [12] discovered the breakdown of the area theorem for the few-cycle pulses of large area ($2\pi n$ with $n \geq 3$), while for lower areas this theorem is still able to predict the profile change of the pulse accompanied by its splitting [13]. Later Tarasishin *et al.* [3] reported that the half- and quarter-cycle 2π pulses leave some small residual excitation inside the two-level medium. Here we show that these deviations from the area theorem are much more noticeable at larger areas of the incident subcycle pulses and we trace appearance of the theorem breakdown with a shortening of the pulse. Moreover, these deviations appear to be strongly dependent on the pulse shape. The effect of pulse form on the excitation probability of the two-level system is known for nonresonant excitation (see, for example, the work by Conover [14] and references therein). However, we consider strictly resonant pulses, their shape being important only for the number of cycles less than unity.

The structure of the paper is as follows. In Section II we establish the Maxwell–Bloch equations to be numerically solved and give the main parameters of calculations. In Section III, comparing our results with the results known from the literature, we prove that the method based on the equations stated in the previous section can be applied to simulate ultrashort pulse propagation beyond the RWA and SVEA. Section IV is devoted to the study of subcycle pulse interaction with the two-level medium, namely to the issues of the area theorem breakdown and the influence of pulse shape. Finally, in Section V we give a short conclusion.

II. MAIN EQUATIONS AND PARAMETERS

Light propagation in the two-level medium beyond the RWA and SVEA is given by the Maxwell–Bloch equations

* dvnovitsky@tut.by

as follows [2, 15]:

$$\frac{\partial^2 E}{\partial z^2} - \frac{1}{c^2} \frac{\partial^2 E}{\partial t^2} = \frac{4\pi}{c^2} \frac{\partial^2 P}{\partial t^2}, \quad (1)$$

$$\frac{d\rho_{12}}{dt} = i\omega_0\rho_{12} + i\frac{\mu}{\hbar}Ew - \gamma_2\rho_{12}, \quad (2)$$

$$\frac{dw}{dt} = -4\frac{\mu}{\hbar}E\text{Im}\rho_{12} - \gamma_1(w + 1), \quad (3)$$

where E is the electric field of a light wave, ρ_{12} the off-resonant density matrix element (atomic polarization), $w = \rho_{22} - \rho_{11}$ the inversion (population difference), ω_0 the frequency of atomic resonance, μ the dipole moment of the quantum transition, γ_1 and γ_2 the rates of relaxation of population and polarization, respectively, c the speed of light, and \hbar the Planck constant. Here the macroscopic polarization of the two-level medium is $P = 2\mu C\text{Re}\rho_{12}$ with C as the concentration (density) of two-level atoms. The symbols Re and Im stand for taking of real and imaginary parts, respectively.

Our aim is to rewrite Eqs. (1) to (3) in such a manner that they would allow direct comparison of the calculations conducted with and without the RWA in the framework of a single numerical algorithm. To reach this aim, we represent the electric field and atomic polarization as $E = \{A \exp[i(\omega t - kz)] + \text{c.c.}\}/2$ and $\rho_{12} = p \exp[i(\omega t - kz)]$, respectively, but the complex amplitudes A and p are not assumed to be slowly varying. Here ω is the central frequency of radiation, $k = \omega/c$ is the wavenumber, and c.c. stands for complex conjugated term. Introducing dimensionless arguments $\tau = \omega t$ and $\xi = kz$ and the dimensionless field amplitude $\Omega = (\mu/\hbar\omega)A$ (normalized Rabi frequency), we come to the set of equations

$$\begin{aligned} \frac{\partial^2 \Omega}{\partial \xi^2} - \frac{\partial^2 \Omega}{\partial \tau^2} - 2i \frac{\partial \Omega}{\partial \xi} - 2i \frac{\partial \Omega}{\partial \tau} \\ = 6\epsilon \left(\frac{\partial^2 p}{\partial \tau^2} + 2i \frac{\partial p}{\partial \tau} - p \right), \end{aligned} \quad (4)$$

$$\frac{dp}{d\tau} = i\delta p + \frac{i}{2}(\Omega + s\Omega^* e^{-2i(\tau-\xi)})w - \gamma_2' p, \quad (5)$$

$$\begin{aligned} \frac{dw}{d\tau} = i(\Omega^* p - \Omega p^*) + is \left(\Omega p e^{2i(\tau-\xi)} - \Omega^* p^* e^{-2i(\tau-\xi)} \right) \\ - \gamma_1'(w + 1), \end{aligned} \quad (6)$$

where $\delta = \Delta\omega/\omega = (\omega_0 - \omega)/\omega$ is the frequency detuning, $\gamma_{1,2}' = \gamma_{1,2}/\omega$ are the normalized relaxation rates, and $\epsilon = \omega_L/\omega = 4\pi\mu^2 C/3\hbar\omega$ is the dimensionless parameter of interaction between light and matter (or normalized Lorentz frequency). Finally, the auxiliary two-valued coefficient s marks the situation considered: $s = 0$ corresponds to the RWA (absence of ‘‘rapidly rotating’’ terms), while $s = 1$ is related to the general case. In this paper we numerically solve Eqs. (4) to (6), so that we have the possibility of switching between the general (non-RWA)

and RWA cases by simply choosing the appropriate value of the single parameter. The numerical approach is essentially the same as in our previous publications [16–19] where the relatively long pulses were studied in the limit of the RWA (but not the SVEA in the wave equation). Therefore, we do not discuss the details of the method and refer the reader to those works.

We adopt the following parameters of the medium and light throughout the paper: the relaxation rates $\gamma_1 = 1$ and $\gamma_2 = 10 \text{ ns}^{-1}$ are large enough so that we are in the regime of coherent light-matter interaction; the detuning $\delta = 0$ (exact resonance); the light wavelength $\lambda = 2\pi c/\omega = 0.83 \text{ }\mu\text{m}$; and the strength of light-matter coupling $\omega_L = 10^{11} \text{ s}^{-1}$ which is much less than the radiation frequency. These material parameters mean that one needs to take relatively long thicknesses of the two-level medium ($L \gg \lambda$) to observe the transformations of the few- or subcycle pulse envelope. Therefore we do not discuss here the effects of pulse profile changing considered previously for the relatively stronger coupling conditions ($\omega_L \sim 10^{12} - 10^{13} \text{ s}^{-1}$) [2, 3, 12]. Moreover, in the strong coupling limit, when the peak Rabi frequency $\Omega_0\omega$ is comparable to or less than the Lorentz frequency, one needs to take into account the so-called local field effects [17]. In our research we can neglect them, since the opposite inequality takes place ($\Omega_0\omega \gg \omega_L$). The estimation shows that a single-cycle 2π soliton in a collection of two-level atoms with dipole moments $\mu \sim 1 \text{ D}$ should have the peak amplitude of about 0.4 GV/cm . The required concentration in this case is $C \approx 2 \times 10^{19} \text{ cm}^{-3}$. Obviously, the results of the calculations can be rescaled for another set of parameters without loss of generality.

In this paper we consider the pulses of two different shapes: the hyperbolic secant $\Omega = \Omega_p \text{sech}(t/t_p)$ and Gaussian $\Omega = \Omega_p \exp(-t^2/2t_p^2)$. The duration of the pulse t_p is defined through the number of cycles N as $t_p = NT/f$, where $T = \lambda/c$ is the period of electric field oscillations, and f is the coefficient which depends on the pulse form and describes its full width at half maximum (FWHM). For the hyperbolic secant pulse we have $f = 2\text{arccosh}\sqrt{2}$, while for the Gaussian shape $f = 2\sqrt{\ln 2}$. The peak (normalized) Rabi frequency Ω_p is measured in the units of Ω_0 corresponding to the area of 2π , so that for the hyperbolic secant pulse one should take $\Omega_0 = \lambda/\pi c t_p$ and for the Gaussian pulse $\Omega_0 = \lambda/\sqrt{2\pi} c t_p$. The calculational region includes the two-level medium of thickness L surrounded by the vacuum regions of length $0.64 \text{ }\mu\text{m}$. The medium is supposed to be initially in the ground state ($w = -1$).

III. TESTING THE CALCULATION APPROACH

First of all, we need to ascertain that the method based on solving of Eqs. (4) to (6) correctly describes propagation of the light pulses in the two-level medium. There are two such tests that are to be considered further.

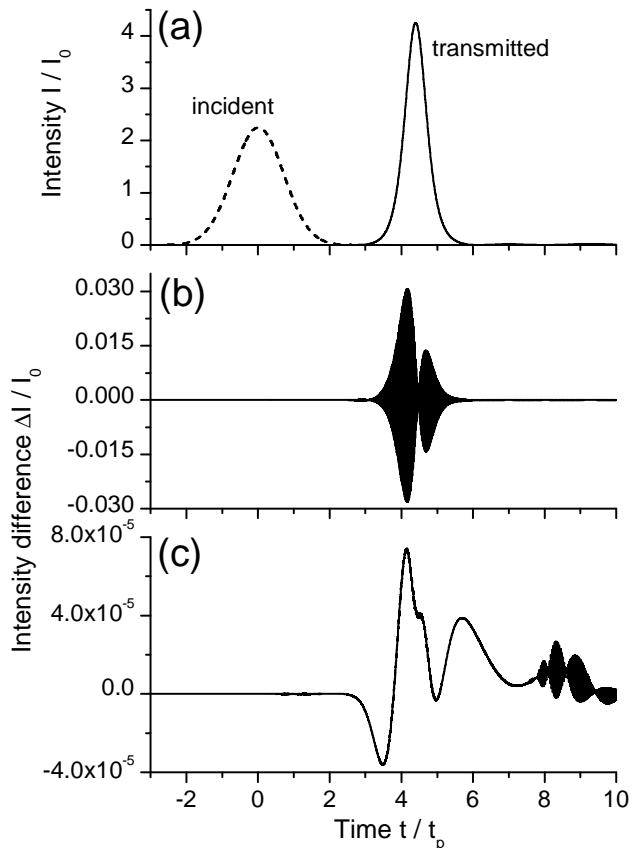


FIG. 1. (a) The profile of the Gaussian 50-cycle 3π pulse transmitted through the two-level medium of length $L = 100\lambda$. Calculations were carried out for the general case ($s = 1$). (b) The difference between the intensity profiles obtained for $s = 1$ and $s = 0$. (c) The difference between the intensity profiles calculated by two different RWA schemes: the scheme of Eqs. (4) to (6) at $s = 0$ and that of Ref. [16]. Intensities are normalized by $I_0 = \Omega_0^2$.

(i) *The limit of long pulses.* In this situation one expects that the calculations at $s = 1$ and $s = 0$ give approximately the same result. To prove these expectations, we launch the Gaussian 3π pulse of 50 cycles (the duration $t_p \approx 83$ fs) into the two-level medium of thickness $L = 100\lambda = 83 \mu\text{m}$. We also carry out the calculations according to the numerical scheme of Ref. [16] to check the consistency with the RWA case realized in our previous works [16–19]. Figure 1(a) shows the intensity profile of such a long pulse transmitted through the layer of thickness $L = 100\lambda$; calculations were performed by Eqs. (4) to (6) at $s = 1$. One of the main features of such a long pulse dynamics is seen: the pulse is compressed while forming the constant-form soliton [18]. Simulations of the RWA scheme show the agreement with the profile of Fig. 1(a). The plots in Figs. 1(b) and 1(c) demonstrate the accuracy of this agreement: the difference between the intensity profiles obtained for $s = 1$ and $s = 0$ is as low as several hundredth of I_0 (the unit of intensity equal to Ω_0^2), while the discrepancy between

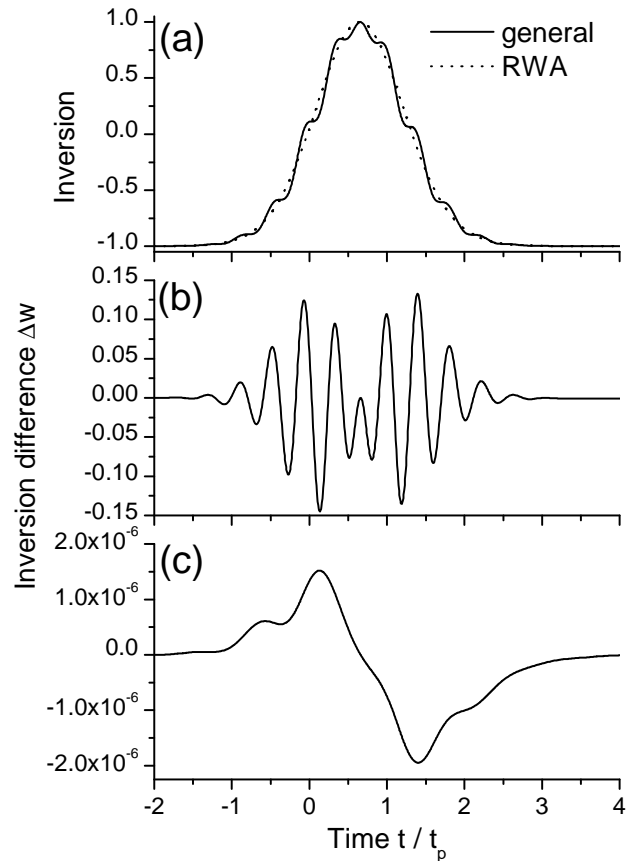


FIG. 2. (a) Dynamics of the inversion at the entrance of the two-level medium excited by the Gaussian two-cycle 2π pulse. Calculations were carried out both for the general case ($s = 1$) and for the RWA ($s = 0$). (b) The difference between the inversion profiles obtained for $s = 1$ and $s = 0$. (c) The difference between the inversion profiles calculated by two different RWA schemes: the scheme of Eqs. (4) to (6) at $s = 0$ and that of Ref. [16].

the calculations by two RWA schemes does not exceed $10^{-4}I_0$, respectively. This proves the correctness of our approach in the long pulse limit.

(ii) *Behavior of inversion in the case of a few-cycle pulse.* Since the shape of the few-cycle pulse varies too slowly as it propagates, our second test deals with the time variation of the inversion w at the entrance of the two-level medium. To excite the medium, the two-cycle 2π Gaussian pulse is used (its duration is about 3.32 fs). The results of calculations are demonstrated in Fig. 2. The difference between $s = 1$ and $s = 0$ cases is clearly seen and reaches values as large as 0.15. The inversion profile calculated without the RWA shows also the feature characteristic for the few-cycle pulse propagation – the step-like flattenings corresponding to the extremes of the time derivative of the electric field [1]. Finally, Fig. 2(c) is the evidence of the precise correspondence between the calculation at $s = 0$ and the RWA calculations according to the previously used approach. Thus, we conclude that our numerical method based on Eqs. (4) to (6) allows one

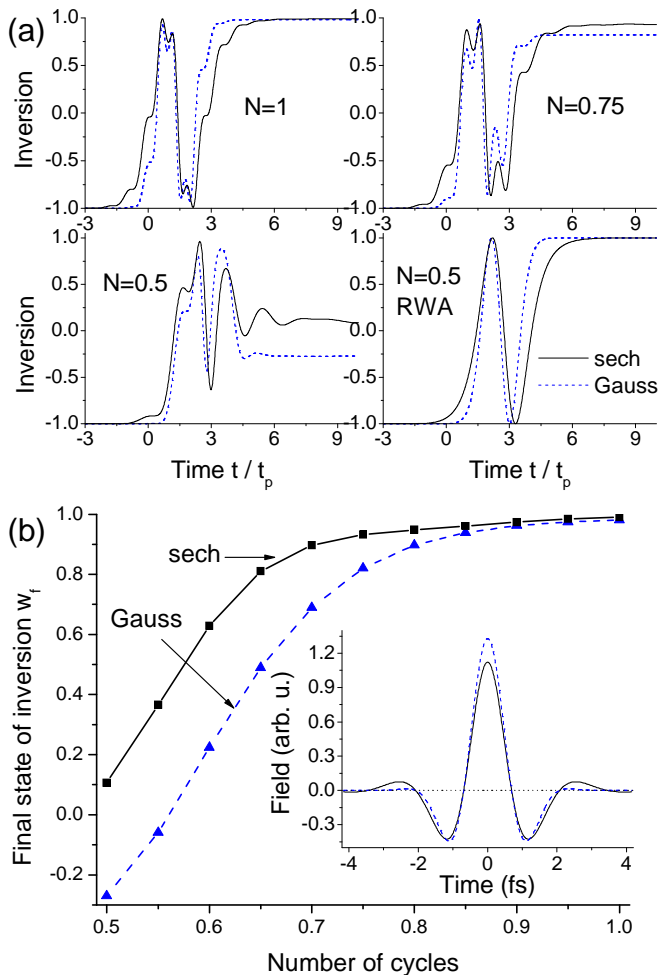


FIG. 3. (Color online) (a) Dynamics of the inversion at the entrance of the two-level medium excited by the Gaussian and hyperbolic secant 3π pulses of different numbers of cycles N . (b) The corresponding dependence of the final state of inversion (FSI) w_f on the number of cycles. FSI was determined at the time point $t = 50t_p$. The inset shows the field profiles of the half-cycle 3π pulses of the Gaussian and sech shapes.

to reproduce the main peculiarities of long- and short-pulse propagation discovered previously and can be used to study the subcycle pulses beyond the RWA.

IV. RESULTS ON SUBCYCLE PULSES

Let us apply the method described above to simulate propagation of subcycle pulses in the two-level medium. The main parameter to be traced is the final state of inversion (FSI) denoted here by w_f . It is the steady value of inversion in which the medium appears after passage of the incident pulse. The area theorem implies that FSI depends on the pulse area: if the starting state of inversion is $w_s = -1$ (two-level system in the ground state), then for the pulse area $n\pi$ one will have $w_f = 1$ or -1 at odd and even values of integer n . Figure 3(a)

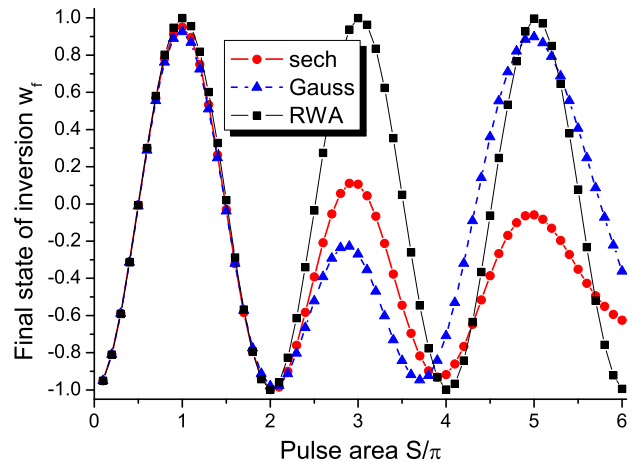


FIG. 4. (Color online) The dependence of the final state of inversion (FSI) w_f on the area of the half-cycle pulses of the Gaussian and hyperbolic secant shapes. The results for the RWA case are given for comparison. FSI was determined at the time point $t = 50t_p$.

shows the dynamics of inversion at the entrance of the two-level medium under the influence of the 3π subcycle pulse, i.e. for the number of cycles $N \leq 1$. It is seen that for the single-cycle pulse ($N = 1$) the FSI approximately (though not exactly) corresponds to the value predicted by the area theorem ($w_f = 1$). As the duration of the pulse decreases ($N = 0.75$ and 0.5), the breakdown of the area theorem becomes apparent: such a short pulse simply cannot guarantee the full cycle of inversion dynamics, so that w finally appears somewhere in between -1 and 1 . The concrete value of w_f strongly depends on the pulse shape. We considered two different variants – secant hyperbolic and Gaussian pulses – and see that the difference between the FSI in these two variants grows as the pulses become shorter. For comparison, we also calculated the RWA curves for the half-cycle pulses [see the lower right panel in Fig. 3(a)]. In this case the area theorem is strictly valid for the pulses of any shape. In other words, the importance of the rapidly rotating terms in the Bloch equations increases for ultrashort pulses and results not only in the breakdown of the area theorem, but also in the strong dependence of the medium dynamics on the pulse form. This is seen in the dependence of w_f on the number of cycles N shown in Fig. 3(b): for the Gaussian subcycle pulses, w_f deviates faster from the area theorem than in the case of sech pulses. This result seems to be rather surprising, since the field profiles of sech and Gaussian half-cycle pulses seem to be not so much different (see the inset) to lead to such a large difference in w_f ($\Delta w_f \approx 0.35$). Thus, in the range of subcycle pulses, even a small distinction in the pulse shape may result in a strong change of the medium dynamics. This should be taken into account when performing experiments with subcycle pulses and gives an additional parameter to control the state of the medium.

The next issue is the dependence of the above described

breakdown of the area theorem on the pulse area. Let us calculate the FSI for different areas of the incident half-cycle pulse ($N = 0.5$). The results for the Gaussian and hyperbolic secant forms are presented in Fig. 4 as well as the RWA data which are the same for both pulse profiles. It is seen that at small areas all three curves approximately coincide and only small deviations from the area theorem occur as was reported previously [3]. But at the areas above 2π the curves rapidly diverge, so that the large-area half-cycle pulses carry the medium to the state with the level population which depends on the shape of the pulse. Moreover, the positions of minima and maxima of inversion also shift from the usual values. This is especially clearly seen for the second minimum: while it is the area of 4π in the RWA case, it is significantly lower in the general case – about 3.9π for the hyperbolic secant pulse and even 3.7π for the Gaussian one. It is also worth noting that the curve for the sech shape is closer to the RWA dependence in the vicinity of 3π areas, but the situation turns out to be opposite in the vicinity of 5π where the curve for the Gaussian pulse approaches the values consistent with the area theorem. The need of large areas ($\geq 2\pi$) to observe the strong deviations from the area theorem can be explained by the fact that the medium affected by the subcycle pulse does not have enough time to develop the full cycle of dynam-

ics when it includes more than a single excitation and deexcitation.

V. CONCLUSION

In summary, we have implemented and tested the numerical approach which allows one to solve the Maxwell–Bloch equations beyond the RWA and SVEA. This method was used to study the effects of the interaction of the subcycle pulses with the two-level medium. For such pulses containing less than one period of optical field, we have found that (i) the breakdown of the area theorem becomes apparent at areas larger than 2π , and (ii) the result of light-matter interaction strongly depends on the pulse shape. Our research was focused on the study of the medium dynamics so that we have not considered the effects of subcycle pulse profile change such as the formation of an asymmetric wave form [3]. Another interesting issue worth to be studying further is the possibility or impossibility of subcycle self-induced-transparency (SIT) solitons. On the one hand, there are studies that show the existence of few-cycle SIT solitons [20]. On the other hand, the attempts to find a solitonic regime for subcycle pulses were not successful so far [3]. The approach reported in this paper can be used for a detailed study of this question.

-
- [1] R. W. Ziolkowski, J. M. Arnold, and D. M. Gogny, *Phys. Rev. A* **52**, 3082 (1995).
 - [2] V. P. Kalosha and J. Herrmann, *Phys. Rev. Lett.* **83**, 544 (1999).
 - [3] A. V. Tarasishin, S. A. Magnitskii, V. A. Shuvaev, and A. M. Zheltikov, *Opt. Express* **8**, 452 (2001).
 - [4] K. Xia, S. Gong, C. Liu, X. Song, and Y. Niu, *Opt. Express* **13**, 5913 (2005).
 - [5] C. Zhang, W. Yang, X. Song, and Z. Xu, *Opt. Express* **17**, 21754 (2009).
 - [6] X.-T. Xie and M. A. Macovei, *Phys. Rev. Lett.* **104**, 073902 (2010).
 - [7] A. Pusch, J. M. Hamm, and O. Hess, *Phys. Rev. A* **84**, 023827 (2011).
 - [8] S. Ibáñez, A. Peralta Conde, D. Guéry-Odelin, and J. G. Muga, *Phys. Rev. A* **84**, 013428 (2011).
 - [9] A. Pusch, J. M. Hamm, and O. Hess, *Phys. Rev. A* **85**, 043807 (2012).
 - [10] Q. Q. Xu, D. Z. Yao, X. N. Liu, Q. Zhou, and G. G. Xiong, *Phys. Rev. A* **86**, 023853 (2012).
 - [11] Ni Cui and M. A. Macovei, *New J. Phys.* **14**, 093031 (2012).
 - [12] S. Hughes, *Phys. Rev. Lett.* **81**, 3363 (1998).
 - [13] J. Xiao, Z. Wang, and Z. Xu, *Phys. Rev. A* **65**, 031402(R) (2002).
 - [14] C. W. S. Conover, *Phys. Rev. A* **84**, 063416 (2011).
 - [15] L. Allen and J.H. Eberly, *Optical Resonance and Two-Level Atoms* (Wiley, New York, 1975).
 - [16] D. V. Novitsky, *Phys. Rev. A* **79**, 023828 (2009).
 - [17] D. V. Novitsky, *Phys. Rev. A* **82**, 015802 (2010).
 - [18] D. V. Novitsky, *Phys. Rev. A* **84**, 013817 (2011).
 - [19] D. V. Novitsky, *Phys. Rev. A* **85**, 043813 (2012).
 - [20] Y. Y. Lin, I-H. Chen, and R.-K. Lee, *Phys. Rev. A* **83**, 043828 (2011).